

Density-of-states fine structure in the tunneling conductance of Y-Ba-Cu-O films: A comparison between experiment and theory

T. G. Miller, M. McElfresh, and R. Reifenberger

Department of Physics, Purdue University, West Lafayette, Indiana 47907

(Received 23 April 1993)

With improved signal-averaging techniques, the tunneling conductance from pulsed-laser-deposited films of $\text{YBa}_2\text{Cu}_3\text{O}_{7-\delta}$ reveals a rich fine structure in both the subgap and near-gap regions. A comparison of this structure with calculations by Tachiki *et al.* yields excellent agreement and indicates the origin of the fine structure is the density of electronic states on the different layered planes of this high- T_c material.

I. INTRODUCTION

The study of Y-Ba-Cu-O by scanning tunneling microscopy (STM), although initially difficult, has provided a number of interesting results. Hawley *et al.*¹ and Gerber *et al.*,² as well as a number of other groups,³⁻⁶ have succeeded in scanning *c*-axis-oriented thin films of Y-Ba-Cu-O with sufficient vertical resolution to easily identify unit-cell-sized features. Atomic-resolution images at room temperature have been obtained by Lang, Frey, and Güntherodt.³ More recently, Edwards, Markert, and de Lozanne⁷ have succeeded in obtaining low-temperature atomic-resolution images. Taken together, these results have demonstrated the utility of STM for studying the surface morphology of high- T_c materials.

Position-sensitive spectroscopy has been more difficult, with the best early results obtained by point-contact junctions.^{8,9} Tunneling measurements in Y-Ba-Cu-O have produced a variety of results,¹⁰ and the most recent evidence suggests a superconducting gap of ~ 20 meV. Evidence for subgap and near-gap structures in Y-Ba-Cu-O tunnel junctions has also been reported.¹¹ Here we report the results of a study on pulsed-laser-deposited Y-Ba-Cu-O films with a low-temperature STM. We obtain conductance data [$G(\text{eV}) = dI/dV$] that are rich in fine structure. This structure, when compared to the tunneling conductance based on a band-structure calculation of Y-Ba-Cu-O by Tachiki *et al.*,²⁵ confirms that we are observing effects due to the Y-Ba-Cu-O density of states. The agreement between experiment and theory provides insight into the factors influencing the tunneling of current into high- T_c materials.

II. EXPERIMENTAL DETAILS

The films studied were prepared by pulsed laser deposition using methods previously described.^{12,13} The films were *c*-axis oriented with thicknesses of ~ 150 nm and were deposited on the (100) plane of LaAlO_3 single-crystal substrates. Magnetization measurements indicated that the films were of high quality, with supercon-

ducting transition temperatures greater than 90 K and $J_c > 10^6$ A/cm² at zero field.

A major obstacle to obtaining consistent spectroscopic and topographic data, particularly at low temperatures, is the difficulty in maintaining adequate surface quality. Numerous studies have indicated that the Y-Ba-Cu-O surface is reactive.¹⁰ One way to avoid contamination is to cleave under UHV conditions.⁷ As described below, we find that handling samples in an inert gas atmosphere is also sufficient to allow high-quality tunneling results. The technique for handling the films is as follows. After deposition and *in situ* annealing, the films were removed from the growth chamber and inserted into a desiccator, which was then transferred into a Vacuum Atmospheres glove box through a load lock.

The glove box was maintained with an inert nitrogen atmosphere.¹⁴ Electrical contact to the samples was made with silver-loaded paint.¹⁵ The sample was mounted in the low-temperature STM and then removed from the glove box and transferred immediately into a vacuum-tight insert Dewar under ambient conditions. This insert Dewar was then quickly evacuated prior to immersion into a liquid-helium storage Dewar supported on a vibration-isolation platform. Following this procedure, total exposure to ambient conditions was kept under 20 s.

The STM used for these studies was constructed to operate at low temperatures and is similar to previously published designs.¹⁶⁻¹⁸ A coarse approach is achieved through an inertial sliding mechanism as described by Renner *et al.*¹⁷ STM tips were formed from cut PtIr wires (0.25 mm diameter). Images were taken with biases of about ± 1.5 V and tunnel currents of approximately 1 nA. High-quality images consistently showed unit-cell terracing at 4.2 K. Scanning was performed utilizing a computer-controlled digital feedback system.¹⁹ A Keithley current amplifier (model 428) with a gain of 10^9 - 10^{10} V/A was used to amplify the tunnel current.

Topographical studies at both room temperature and 4.2 K revealed a surface morphology consisting of large areas of stacked-disk-type structures. This type of terracing indicates that an island growth mechanism is primarily responsible for film growth. Figure 1 is a small-scale

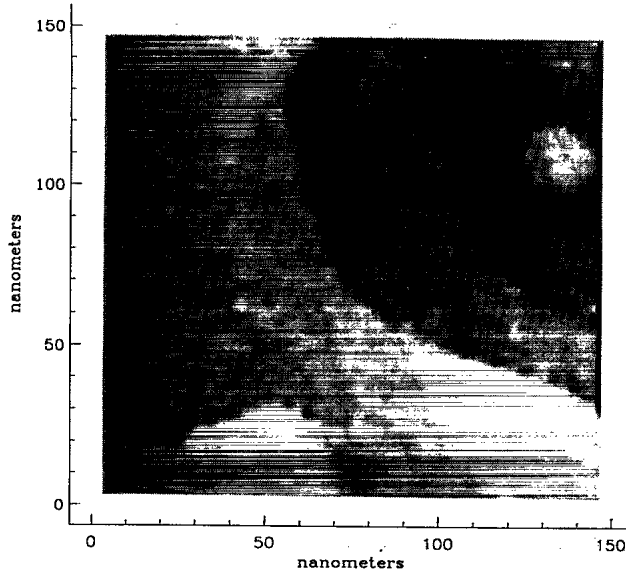


FIG. 1. Top view image of a Y-Ba-Cu-O thin film taken at 4.2 K. Unit-cell terracing with steps of one unit cell (1.2 nm) high are visible.

scan taken at 4.2 K showing some terrace steps. The flat terraces with step heights of exactly one unit cell (1.2 nm) confirm that the region being studied was well c -axis oriented. Analysis of data taken on different grains indicated at most a 1° – 2° mismatch between the c -axis orientation of different grains.

A quantitative technique for analyzing the terracing in an entire image is to make a histogram of surface heights. Figure 2 is a plot of the percentage of points on the sur-

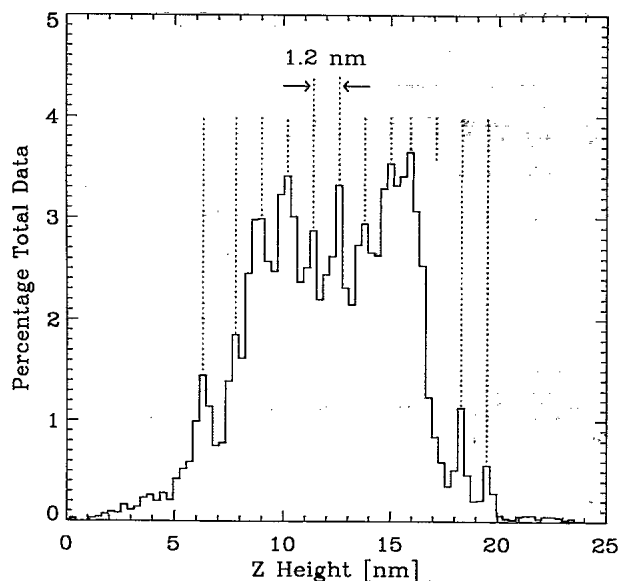


FIG. 2. Histogram plot of the pixel heights from a highly terraced region of a Y-Ba-Cu-O film as a percentage of the total image. The spacing between peaks (dashed lines) is predominantly one c -axis unit cell in distance (1.2 nm).

face as a function of height. This data was from a $1.5 \times 1.5 \mu\text{m}$ scan taken at 4.2 K. An advantage of this approach is that information about the terracing of the entire film can be readily obtained. All but two of the peak-to-peak spacings indicated by dotted lines in Fig. 2 are one c -axis unit cell high. Nonepitaxial films, or regions of the film with a -axis or disordered growth, can easily be identified by a lack of peak structure in the histogram.

III. RESULTS

A. Tunnel gap quality

We have found that a measurement of the tunneling current as a function of tip height is a particularly effective way to characterize the quality of the film surface. The exponential decay of tunnel current with distance is a well-known result of all tunneling models and is specified by

$$I(z) = I_0 e^{-1.025\sqrt{\bar{\phi}} z}, \quad (1)$$

where I is the tunnel current, z is the distance between the tip and sample (in angstroms), and $\bar{\phi}$ is the effective barrier height (in eV) of the tunnel junction. This generally accepted model predicts tunnel currents dropping off to negligibly small values for $z \sim 10 \text{ \AA}$.²⁰ Tunnel junctions formed in air, however, often are much less than ideal. This departure from theoretical expectations is usually attributed to surface contamination.

The distance over which the tunnel current falls off is a quantitative measure of the tunnel junction quality and can be used to study the effect of exposure to ambient conditions on Y-Ba-Cu-O thin films. Figure 3 shows typical data for the tunnel current versus tip-sample separation. The solid curve shows $I(z)$ obtained from a Y-Ba-Cu-O film handled in the way described previously while the dotted $I(z)$ curve was obtained after an 8-min exposure to air. Analysis of the data from the unexposed sample using Eq. (1) (see inset in Fig. 1) gives a tunnel barrier height of 0.8 eV, in reasonable agreement with values recently reported on vacuum cleaved samples.⁷

Upon exposure to air, the $I(z)$ spectra changed dramatically, with significant tunnel currents still present after withdrawing the tip 200 \AA . The surface of Y-Ba-Cu-O is well known to be unstable and tends to form an insulating layer, often attributed to the presence of adsorbed water on the surface.¹⁰ The $I(z)$ curve for the exposed sample is not logarithmic, and thus it is not possible to obtain a barrier height from it. An important conclusion drawn from this analysis is that we can readily determine when vacuum tunneling conditions have been achieved.

B. Tunneling conductance

After verifying that vacuum tunneling had been established, conductance studies were performed at 4.2 K by first selecting a desired region of the film from STM topo-

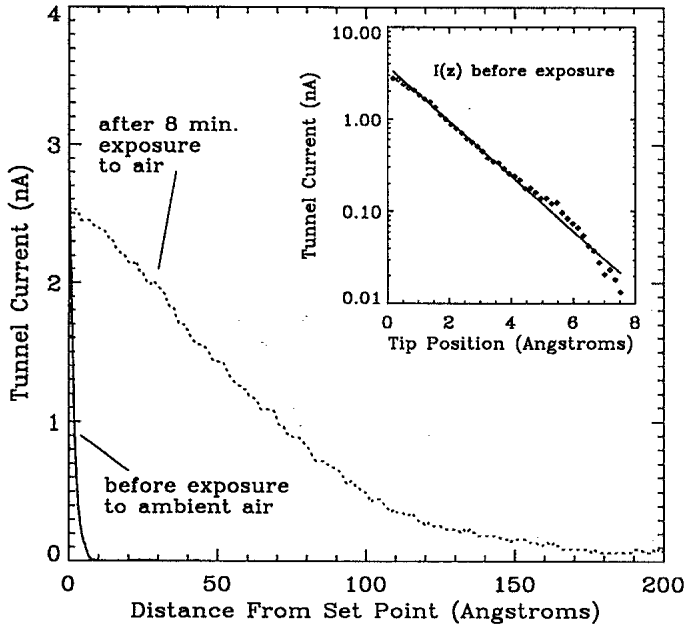


FIG. 3. Plot of the tunnel current from a Pt-Ir tip into a pulsed-laser-deposited Y-Ba-Cu-O film at room temperature as a function of tip-sample separation. The solid curve was taken after mounting the sample onto the STM in an inert-atmosphere glove box. The dotted curve is the tunnel current measured at the same position after an 8-min exposure to ambient air. The inset is plot of the logarithm of the tunnel current into the unexposed film as a function of the tip-sample separation. From Eq. (1), the slope of this data can be related to the tunnel barrier height.

graphic scans. $I(V)$ measurements were made in which the computer feedback was paused, and the tip bias was ramped over the desired voltage range while the tunneling current was digitized. After one sweep, the feedback was momentarily enabled and the tip-sample separation was checked and adjusted in the usual way. Total acquisition time for each sweep was 75 ms or less. Using this technique, a preset number of $I(V)$ curves taken at a predetermined point on the sample could be averaged together. The derivative of the final $I(V)$ curve was obtained numerically. We have found that the flexibility inherent in digital feedback offers a number of advantages over analog feedback schemes such as asynchronous operation and the elimination of glitches associated with sample-and-hold circuits.

In general, the $I(V)$ curves from different regions of the thin films showed a variety of different behaviors.²¹ Evidence for linear conductance was often obtained. An apparent Coulomb blockade, evident from a current suppression near zero bias voltage, was also occasionally seen. Conductance curves characterized by a recognizable superconducting energy gap were also found. An example of this latter data is shown in Fig. 4.

In Fig. 4, we plot the normalized conductance, defined as $[(dI/dV)_s / (dI/dV)_n]$, obtained at 4.2 K from a region of the Y-Ba-Cu-O film characterized by well-formed terraces. For this data, the STM was operated with a tunnel resistance of ~ 4 G Ω . The normal-state conductance

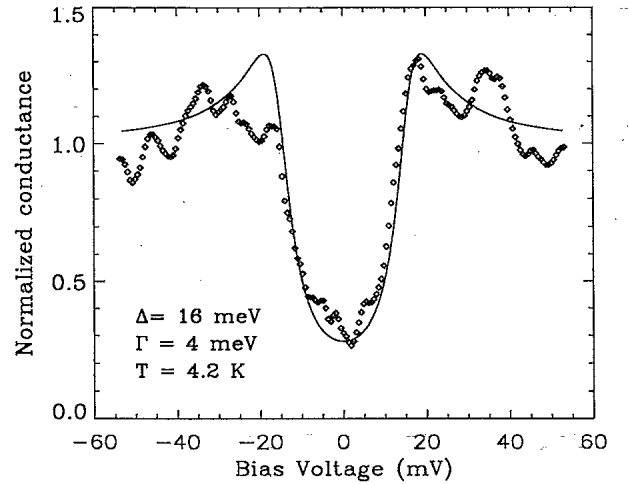


FIG. 4. Plot of the normalized conductance as a function of the tip bias voltage obtained from a Y-Ba-Cu-O film at 4.2 K. The solid line is a fit to the data using the model of Dynes *et al.* (Ref. 24) [Eq. (2)].

was approximated from the $I(V)$ data far from the gap region (60 mV). This data represent an average of 1024 sweeps. The large amount of averaging increases confidence that any structure observed is not an electronic artifact since the sweeps are asynchronous with each other. Apart from the appearance of a well-characterized gap feature, considerable subgap and near-gap structures are also observed. The number of sweeps required to make the fine structure clearly evident was dictated by hints of reproducible structure obtained after averaging a smaller number of sweeps. We find that the conductance at $V_{\text{bias}} = 0$ is about 30% of the conductance at 60 mV. Because of this excessive subgap conductance, an analysis of this data with a standard BCS quasiparticle density of states yields a poor fit.

An important issue to address is the reproducibility of the structure in the conductance data. Figure 5 shows two different curves taken 40 min apart at the same region on the sample. Although the reproducibility is not perfect, the main features of the structure are clearly reproduced. This structure was not necessarily present at every region on the film, an observation suggesting that local variations in stoichiometry may be an important factor in determining the fine structure. It was also observed that the fine structure was more readily seen at large tip-to-sample spacings.

Many studies have observed a smearing of the gap conductance,^{22,23,11} and a common technique is to fit to the data using the model of Dynes *et al.*,²⁴ which predicts a quasiparticle density of states (DOS) of the form

$$\text{DOS}(eV, \Gamma) = \text{Re} \left[\frac{|eV - i\Gamma|}{\sqrt{(eV - i\Gamma)^2 - \Delta^2}} \right], \quad (2)$$

where Δ is the superconducting gap and Γ is an energy broadening parameter due to inelastic-scattering processes. For a high- T_c superconductor, the physical

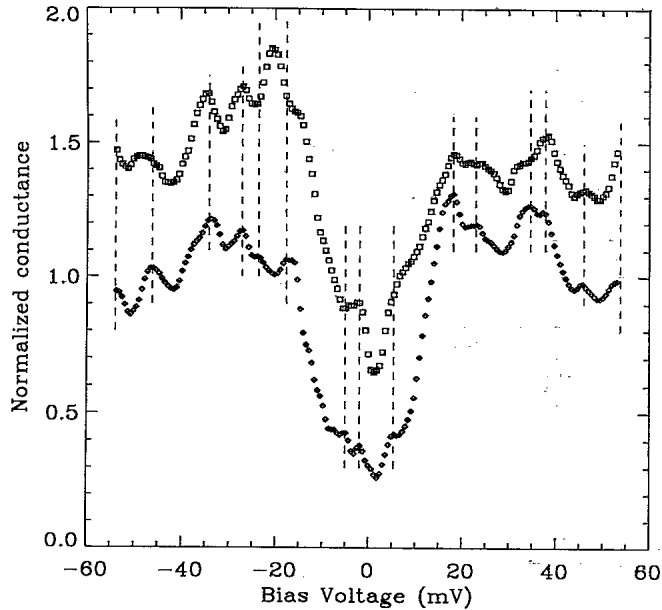


FIG. 5. Two conductance curves taken at the same spot on the sample 40 min apart, illustrating the degree of reproducibility. The dashed lines mark the position of local maxima in the lower curve.

significance of Γ is questionable, but it is a convenient parameter for characterizing the gap. A reasonable fit to the overall shape of our data is given by the solid line in Fig. 4 for $\Gamma=4$ meV, $\Delta=16$ meV. These values can be compared to $\Gamma = 12 \pm 4$ meV and $\Delta = 21 \pm 7$ meV reported by Edwards, Markert, and de Lozanne.⁷

IV. COMPARISON OF FINE STRUCTURE TO THEORY

The model of Dynes *et al.*²⁴ produces no additional structure other than the superconducting gap. An explanation of the fine structure can be obtained by comparing our data to a recent layered band-structure calculation by Tachiki *et al.*²⁵ Using a second-quantization, weak-coupling approach, the Y-Ba-Cu-O material was modeled by a stacked structure of strongly (CuO₂) and weakly (CuO and BaO) superconducting planes as shown in Fig. 6. For simplicity, the spacing between planes was assumed equal. A superconducting pairing interaction was assumed to act only between nearest-neighbor CuO₂ planes. The coupling between planes was specified by three adjustable transfer energies between layers as indicated in Fig. 6. In addition, effective masses for the electrons in each plane were treated as parameters and were fixed ($m_2/m_1 = 0.5$; $m_3/m_1 = 0.75$) by other considerations. The two-dimensional energy bands $\epsilon_1(\vec{k})$, $\epsilon_2(\vec{k})$, $\epsilon_3(\vec{k})$ were calculated and then used to predict the tunneling conductance G_m , $m = 1, 5$ for each plane. For a given tunneling experiment, the conductance for each plane may be weighted differently, and this weighting may be related to the microstructure of the material and the details of the experimental probe.

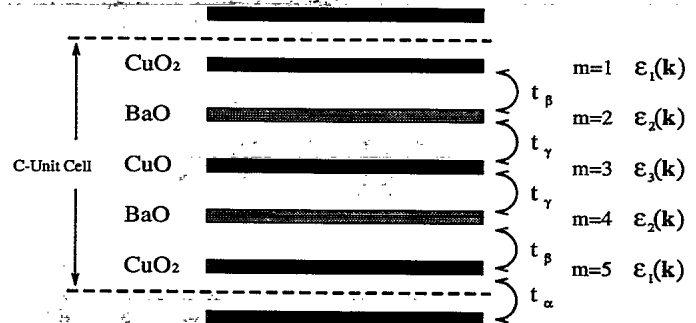


FIG. 6. Schematic of the stacked plane structure used by Tachiki *et al.* (Ref. 25) to calculate the tunneling conductance in Y-Ba-Cu-O. The chemical composition of each plane is indicated, and the interplane coupling parameters t_α , t_β , t_γ are shown schematically.

Tachiki *et al.* calculated the simple case of equal weighting in which the total conductance is given by

$$G_{av} = \frac{1}{5} \sum_{m=1}^5 G_m \quad (3)$$

An important result from this calculation of G_{av} is the prediction of considerable fine structure in the normalized conductance. The fine structure reflects van Hove

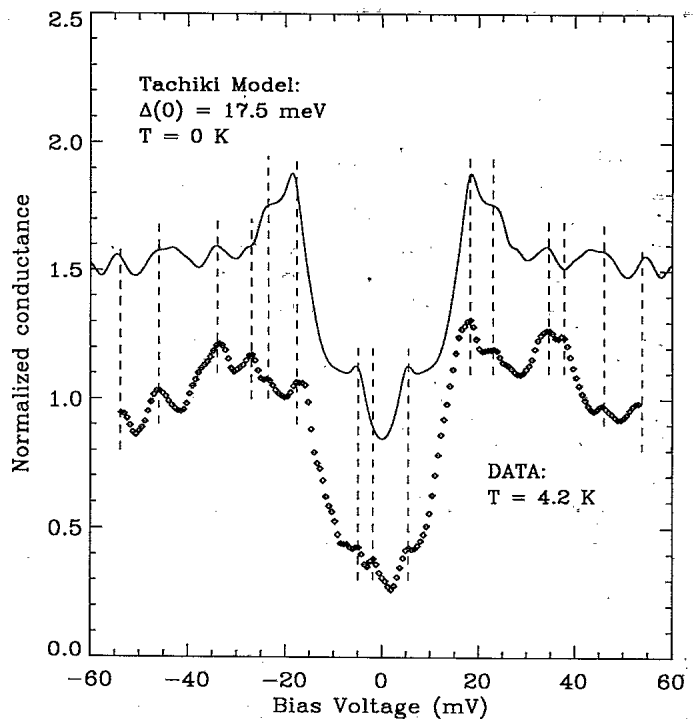


FIG. 7. Comparison between the normalized conductance $[(dI/dV)_s/(dI/dV)_n]$ of a terraced region on Y-Ba-Cu-O at 4.2 K and a theoretical calculation at 0 K by Tachiki *et al.* (see Fig. 5 from Ref. 25). The theoretical curve has been shifted up by 0.5 for clarity. The dashed lines mark the position of local maxima in the experimental data.

singularities in the energy spectrum of the electron states of this layered high- T_c material.

In Fig. 7, we compare our data to the predictions of the model of Tachiki *et al.* For comparison to our data, we did not try for a best fit using different coupling parameters. Instead, the coupling parameters $|t_\alpha| : |t_\beta| : |t_\gamma| = 0.2 : 0.17 : 0.17$ as assumed for Fig. 5 in Ref. 25 were used.

Although no attempts were made to optimize a fit to our data, we find that the position in energy of the peaks predicted by theory is in excellent agreement with our experimental data; of the 15 peaks observed, we find good agreement with 13. It seems likely that better agreement between the details of the fine structure predicted by theory and that observed in our experiment could be further improved by relaxing the simplifying theoretical assumption of equal spacing between the layers in the Y-Ba-Cu-O material used in Ref. 1. Furthermore, the amplitude of the fine structure is in reasonable agreement with the theory. This model predicts a zero-bias conductance of 0.33, which is also in good agreement with our experimental data. From the data, we find evidence for asymmetry in the conductance spectrum that is not predicted by the calculation. This asymmetry has been previously observed and can be attributed to a constant-barrier-height approximation made in the tunneling model.⁹

V. DISCUSSION

Because of the good agreement with the model of Tachiki *et al.*,²⁵ the fine structure observed in the experimental data can be interpreted in more detail. The gap of ~ 17.5 meV in Fig. 3 is due to superconductivity in the CuO₂ plane. The subgap structure at ~ 5 meV is due to the BaO and CuO planes. The additional structure for bias voltages beyond the gap are due primarily to van Hove singularities produced by band crossings of electron states in the BaO and CuO planes. The finite conductance at zero bias is due to gapless excitations in the energy spectrum. The ability to account for all of these details provides evidence that the tunnel current is

strongly influenced by the layered electronic structure of this material.

It follows that not all of the tunneling current is confined to the highly superconducting CuO₂ plane. This might be anticipated since the prevalent island growth morphology observed on pulsed-laser-deposited films may force the tunneling current to pass through coupled layers. It follows that similar fine structure in the conductance may not be observed on cleaved single crystals or films grown by molecular-beam epitaxy. From this discussion, it is also clear that the observed conductance spectrum will depend very sensitively on the coupling of the tunneling probe to the various planes in these high- T_c materials.

VI. SUMMARY

By carefully controlling the surface quality of YBa₂Cu₃O_{7- δ} (Y-Ba-Cu-O) pulsed-laser-deposited thin films and employing improved signal averaging techniques, we find a rich fine structure in the tunneling conductance obtained at 4.2 K with a low-temperature scanning tunneling microscope (STM). The position in energy of this fine structure is in excellent agreement with calculations of Tachiki *et al.*²⁵ This agreement provides insight into how the STM tunneling current is influenced by the surface morphology of the high- T_c films and provides evidence that zero-bias conductance in these materials may be attributed to gapless excitations on the BaO and CuO planes. This result indicates that the STM tunneling current into a *c*-axis-oriented Y-Ba-Cu-O thin film is determined by the collective density of electronic states on the CuO₂, CuO, and BaO layers in the unit cell rather than the superconducting CuO₂ plane alone.

ACKNOWLEDGMENTS

We would like to thank L. Hou, P. Metcalf, and A. Lewicki for their assistance in these studies. This work was supported in part by MISCON under DOE Grant No. DE-FG02-90ER45427.

¹ Marilyn Hawley, Ian D. Raistrick, Jerome G. Beery, and Robert J. Houlton, *Science* **251**, 1587 (1991).

² C. Gerber, D. Anselmetti, J.G.E. Bednorz, J. Mannhart, and D.G. Schlom, *Nature* **350**, 279 (1991).

³ H.P. Lang, T. Frey, and H.J. Güntherodt, *Europhys. Lett.* **15**, 667 (1991).

⁴ David P. Norton, Douglas H. Lowndes, X.Y. Zheng, Shen Zhu, and R.J. Warmack, *Phys. Rev. B* **44**, 9760 (1991).

⁵ John Moreland, Paul Rice, S.E. Russek, B. Jeanneret, A. Roshko, R.H. Ono, and D.A. Rudman, *Appl. Phys. Lett.* **59**, 3039 (1991).

⁶ M. McElfresh, T.G. Miller, R. Reifenberger, R.E. Muenchausen, M. Hawley, S.R. Foltyn, and X.D. Wu, *J. Appl. Phys.* **71**, 5099 (1992).

⁷ H.L. Edwards, J.T. Markert, and A.L. de Lozanne, *Phys.*

Rev. Lett. **69**, 2967 (1992).

⁸ A. Edgar, C.J. Adkins, and S.J. Chandler, *J. Phys. C* **20**, L1009 (1987).

⁹ J.R. Kirtley, S. Washburn, and M.J. Brady, *Phys. Rev. Lett.* **6A**, 1546 (1988).

¹⁰ T. Hasegawa, H. Ikuta, and K. Kitazawa, in *Physical Properties of High Temperature Superconductors III*, edited by D.M. Ginsberg (World Scientific, Singapore, 1992).

¹¹ M. Gurvitch, J.M. Valles, Jr., A.M. Cucolo, R.C. Dynes, J.P. Garno, L.F. Schneemeyer, and J.V. Waszczak, *Phys. Rev. Lett.* **63**, 1008 (1989).

¹² R.E. Muenchausen, K.M. Hubbard, S.R. Foltyn, R.C. Estler, and N.S. Nogar, *Appl. Phys. Lett.* **56**, 578 (1991).

¹³ X.D. Wu, R.E. Muenchausen, S.R. Foltyn, R.C. Estler, R.C. Dye, C. Flamme, N.S. Nogar, A.R. Garcia, J. Martin,

- and J. Tesmen, *Appl. Phys. Lett.* **335**, 1481 (1990).
- ¹⁴ Water-vapor and oxygen levels were below 5 ppm, as determined by titanium(V)-chloride and diethyl-zinc smoke tests.
- ¹⁵ Type SC12 silver paint purchased from Micro-Circuits Co., New Buffalo, Michigan.
- ¹⁶ J.W. Lyding, S. Skala, J.S. Hubacek, R. Brockenbrough, and G. Gammie, *Rev. Sci. Instrum.* **59**, 1897 (1988).
- ¹⁷ Ch. Renner, Ph. Niedermann, A.D. Kent, and O. Fischer, *J. Vac. Sci. Technol. A* **8**, 330 (1990).
- ¹⁸ Ch. Renner, Ph. Niedermann, A.D. Kent, and O. Fischer, *Rev. Sci. Instrum.* **61**, 965 (1990).
- ¹⁹ R. Piner and R. Reifenberger, *Rev. Sci. Instrum.* **60**, 3123 (1989).
- ²⁰ N. Garcia and F. Flores, *Physica* **127B**, 137 (1984).
- ²¹ T.G. Miller, L. Hou, M.W. McElfresh, and R. Reifenberger (unpublished).
- ²² J. Geerk, X.X. Xi, and G. Linker, *Z. Phys. B* **73**, 329 (1988).
- ²³ J. Geerk, G. Linker, O. Meyer, Q. Li, R.L. Wang, and X.X. Xi, *Physica C* **162-64**, 837 (1989).
- ²⁴ R.C. Dynes, J.P. Garno, G.B. Hertel, and T.P. Orlando, *Phys. Rev. Lett.* **53**, 2437 (1984).
- ²⁵ M. Tachiki, S. Takahashi, F. Steglich, and H. Adrian, *Z. Phys. B* **80**, 161 (1990).